REPORT DOCUMENTATION PAGE

Form Approved
OMB NO. 0704-0188

1. AGENCY USE ONLY (Leave Blank)	2. REPORT DATE	3. REPORT TYPE AND DATES COVERED
	04/26/06	Final Progress Report (07/15/02-12/31/05)

4. TITLE AND SUBTITLE

Study of Carrier Dynamics in Self-Assembled InAs QDs and InAs/InGaSb Superlattices using Pump Probe Spectroscopy

5. FUNDING NUMBERS

DAAD19-02-1-0306

6. AUTHOR(S)

Prof. Sanjay Krishna

7. PERFORMING ORGANIZATION NAME(S) AND ADDRESS(ES)

Center for High Technology Materials, University of New Mexico, 1313 Goddard SE, Albuquerque NM 87106

8. PERFORMING ORGANIZATION REPORT NUMBER

Report Number 4

9. SPONSORING / MONITORING AGENCY NAME(S) AND ADDRESS(ES)

U. S. Army Research Office
P.O. Box 12211
Research Triangle Park, NC 27709-2211

10. SPONSORING / MONITORING AGENCY REPORT NUMBER

43806.1-EL-H

11. SUPPLEMENTARY NOTES

The views, opinions and/or findings contained in this report are those of the author(s) and should not be construed as an official Department of the Army position, policy or decision, unless so designated by other documentation.

12 a. DISTRIBUTION / AVAILABILITY STATEMENT

Approved for public release; distribution unlimited.

12 b. DISTRIBUTION CODE

13. ABSTRACT (Maximum 200 words)

The proposed project aims to investigate the carrier dynamics in two systems that are emerging as a promising candidates for mid-wave infrared (MWIR) and long-wave infrared (LWIR) detectors, namely, self assembled InAs/InGaAs quantum dots and InAs/InGaSb strain layer superlattice. In addition to this, a third material system, metamorphically grown "Arsenic Free" (In,Al,Ga)Sb/GaSb materials will also be investigated. The proposed duration of the project is three years. In this period (1st Jan 2003- Dec 31st 2003), metamorphic InGaSb structures were grown and their optical and structural properties were characterized. A femtosecond spectroscopy system was set up to accurately determine the carrier lifetime in all these materials was funded. Results from this grant were published in peer reviewed journals and presented at international conferences.

14. SUBJECT TERMS

Quantum dots, strain layer superlattices, metamorphic buffer, carrier dynamics

15. NUMBER OF PAGES

2

16. PRICE CODE

17. SECURITY CLASSIFICATION OR REPORT	18. SECURITY CLASSIFICATION ON THIS PAGE	19. SECURITY CLASSIFICATION OF ABSTRACT	20. LIMITATION OF ABSTRACT
UNCLASSIFIED	**UNCLASSIFIED**	**UNCLASSIFIED**	**UL**

NSN 7540-01-280-5500

Standard Form 298 (Rev.2-89)
Prescribed by ANSI Std. 239-18
298-102

Enclosure 1

Objective:

To investigate carrier dynamics and relaxation mechanisms in (a) InGaSb metamorphic buffer layers (b) Self Assembled InAs/InGaAs quantum dots and (c) InAs/InGaSb strain layer superlattice with an objective to studying the fundamental limitations for near-infrared and mid-infrared lasers made with these materials.

Progress Report

One of the issues that is being investigated in this grant is to determine (a) whether phonon bottleneck exists in the quantum dots in a well (DWELL) heterostructure and (b) how this impacts the performance of quantum dot lasers. To this end, we are using femtosecond pump probe spectroscopy to understand the carrier dynamics in the DWELL system. A femtosecond spectroscopy set up was installed in the PI's laboratory and very encouraging preliminary measurements have been obtained. Bandstructure calculations were also performed on these structures.

Technical Progress

Non-degenerate pump-probe spectroscopy with sub-picoseconds laser pulses was used to study the carrier dynamics in InAs/InGaAs quantum dots in a well (DWELL) heterostructures. The confined states in the DWELL heterostructure were obtained using theoretical modeling and the position of the ground state was corroborated using differential transmission (DT) and photoluminescence (PL) measuremements. Subpicosecond pump probe spectroscopy was then undertaken using a 775 nm pump to create carriers in the GaAs barrier and a delayed probe tuned to the ground state of the dot (1150 nm). From the rise time of the DT signal, the relaxation time from the GaAs barrier to the ground state of the DWELL was estimated to be 2.5 ps at 77K and 5.0 ps at 300K. The decay of the DT signal was used to determine the interband relaxation time, which was found to be 700 ps at 77K and 650 ps at 300K.

Theoretical Modeling of Bandstructure of QDWELLs.

The study of intersubband transitions in self-assembled quantum dots (QD) has been an area of active research in the past few years. These QDs are not only interesting due to the novel quasi-zero dimensional physics in these systems but also because the interband and intersubband transitions can be utilized to make electronic and optoelectronic devices, that take advantage of the nanoscale confinement in these systems. Due to the long lived excited states and superior carrier confinement, intersubband quantum dot detectors have been proposed as a promising technology for mid infrared sensing (50-400 meV, 3-25 μm). Mid-infrared photodetectors have a variety of potential applications in medical diagnostics, thermal imaging, night vision cameras, and chip-based detection of chemical warfare agents. Detectors based on intersubband transitions in quantum wells have been proposed and realized in the past decade. However, because of polarization sensitive selection rules, normal incidence intersubband transitions are forbidden in such quantum well infrared photodetectors (QWIPs). Moreover, the intersubband carrier relaxation process is expected to be slower in quantum dots than in quantum wells due to suppressed phonon scattering. This effect also known as the "phonon bottleneck process" is predicted for zero-dimensional semiconductor systems which have a discrete density of states

and energy separation greater than the phonon energy separation. Theoretical modeling of pyramidal, cylindrical and hemispherical quantum dots has been performed in the literature using different approaches.. However, while most theoretical models, such as the 8-band **k.p** model predict a separation of 50-60 meV (20-25 μm) between the ground state and the first excited state, most experimental groups report intersubband detectors operating in the 4-7 μm regime.

In our group, we have been investigating intersubband transitions in a novel heterostructure in which InAs quantum dots are placed in an InGaAs well, which in turn is buried in a GaAs matrix. These structures, also known as dots-in-a-well (DWELL) heterostructures, have enabled us to realize long wave infrared detectors (λ_p ~10μm) with low dark currents and high background limited temperatures (91K, f#1.7, 300K bkg).[16] However, the modeling of these detectors has been a challenge since it involves modeling a qausi-zero dimensional QD placed in a 2-dimensional quantum well. In this paper, we report on the modeling of the DWELL structure, using a Bessel function expansion of the wavefunction. The calculated energy levels obtained by this approach are compared with the experimentally observed spectral response of the intersubband detector.

The InAs/InGaAs DWELL detectors were grown by solid source molecular beam epitaxy (MBE). The substrate temperature was 590ºC during the growth of GaAs buffer layer and lowered to 475ºC during the growth of InAs quantum dots. The active region consists of 10 periods of 60Å $In_{0.15}Ga_{0.85}As$, 2.4 monolayers of InAs, 60Å of $In_{0.15}Ga_{0.85}As$ and 490 Å of GaAs (figure 1(a)). The InAs layers are doped with silicon with a concentration of ~5 x 10^{10} atoms/cm^2. The growth rate for the InAs layer is 0.05ML/s. The GaAs contact layer is doped with silicon to 10^{18} cm^{-3}.

Using standard lithography, metal evaporation, and a combination of wet and dry etching, n-i-n detectors were fabricated for top-side illumination with the diameter of the illumination area ranging from 25-300 μm. The detectors were bonded to a leadless chip carrier and spectral measurements were performed using a globar source and a Nicolet Nexus 870 FTIR. Normal incidence radiation configuration was used to measure the photocurrent. All the measurements were performed at a temperature between 30-50K. Cross sectional transmission electron microscopy (X-TEM) measurements were undertaken to characterize the structural quality of the sample. In section III we present the results of the X-TEM study that enabled us to obtain the size and shape of the quantum dots and formulate the DWELL potential for the theoretical studies. The proposed theoretical model, with the underlying assumptions, is then presented. In section IV, the theoretically obtained energy levels are compared with the experimentally observed transitions. Section V discusses the results and summarizes our findings.

Figure 1 shows the TEM image of the DWELL heterostructure. It clearly shows three regions. The darkest region is the InAs quantum dot, which is placed in the $In_{0.15}Ga_{0.85}As$ well and in turn is surrounded by the GaAs region, as labeled in the figure 2. Note that this picture shows that the pyramidal shaped quantum dots, with base dimension of 110 Å and height of 65 Å, are positioned in the top half of the quantum well. Using the information from the TEM image, we have defined the DWELL potential profile, shown in figure 3. Our theoretical model consists of a pyramidal shaped InAs quantum dot with dimension 110Å for the base and 65Å for the height, which is placed in the top half of a 110 Å $In_{0.15}Ga_{0.85}As$ well, which in turn is buried in a GaAs matrix. The modeled structure is very similar to the structure shown in the TEM image.

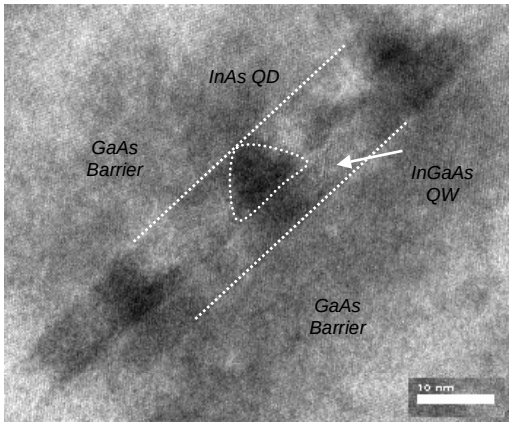

Figure 1: Image of a single quantum dot in a well obtained using cross-sectional transmission electron microscopy.

The numerical approach to the problem consists of enclosing the cluster inside a cylinder of radius R and height Z_c on the surface of which the wavefunctions are forced to vanish. It should be noted that R and Z_c should be made large enough so that we can impose the Dirichlet boundary conditions. In our calculation, we have used Z_c = R = 40nm, although a larger value of Z_c and R does not affect our results. From atomic force microscopy image, the dot density is estimated to be about $5x10^{10}cm^{-2}$. Thus the average spacing between two adjacent dots is about 60 nm. Hence we have ignored lateral coupling between the dots. For determining the bandstructure of the heterostructure, the conduction band offset between the strained InAs and GaAs is taken to be 60% of their difference in band gaps.[17,18] The zero of the potential was chosen as the strained band edge of $In_{0.15}Ga_{0.85}$ and the calculated relative energy E_0 measured from zero reference energy is –146 meV. Since the calculated band offset between InAs and $In_{0.15}Ga_{0.85}As$ is 0.477eV and that between $In_{0.15}Ga_{0.85}As$ and GaAs is 0.093 eV, we found that E_0 is located 268 meV below the band edge of GaAs (Fig.4). Following the notation of figure 3, the electron Hamiltonian is given by:

$$H_e = H_z + H_{(r,\theta)} + V(z,r) \qquad (Eq.1)$$

where

$$H_z = -\frac{\hbar^2}{2}\left(\frac{\partial}{\partial z}\frac{1}{m_e^z(z,r)}\frac{\partial}{\partial z}\right), \qquad (Eq.2)$$

$$H_{(r,\theta)} = -\frac{\hbar^2}{2}\left(\frac{1}{r}\frac{\partial}{\partial r}\frac{r}{m_e^r(z,r)}\frac{\partial}{\partial r} + \frac{1}{m_e^r(z,r)}\frac{1}{r^2}\frac{\partial^2}{\partial\theta^2}\right) \qquad (Eq.3)$$

The overall potential seen by the electron consists of the potential in the three different regions, I, II and III (labeled in Fig. 3) and the potential caused by the external electric field.

$$V(z,r) = V_I(z) + V_{II}(z,r) + V_{III}(z) - eFz \qquad (Eq.4)$$

where

$$V_I(z) = V_{InAs}Y(z - Z_2)Y(Z_3 - z) \qquad (Eq.5)$$

$$V_{II}(z) = V_{InAs}Y(z - Z_3)Y(Z_4 - z)Y[h - (z - Z_3) - r\tan(\alpha)] \qquad (Eq.6)$$

$$V_{III}(z) = V_{GaAs}Y(z)Y(Z_1 - z) + V_{GaAs}Y(z - Z_4)Y(Z_c - z) \qquad (Eq.7)$$

$$V_{IV}(z) = -eFz \qquad (Eq.8)$$

where Y is the Heavyside function, m_e^r and m_e^z are the in-plane and out-of-plane electron effective masses respectively, F is the electric field, which is directed along the z direction (along

the growth axis). Note that there is no term with V_{InGaAs} since the zero of the potential was chosen as the strained band edge of $In_{0.15}Ga_{0.85}As$. The eigenfunctions of the Hamiltonian, given by equation 1, can be decomposed onto the basis formed by the product of Bessel function of integer n with the sine functions of z ,[10] i.e.

$$\chi_n(z,r,\theta) = \sum_{i>0,\, j>0} A_{i,j}^n \xi_{i,j}^n(z,r,\theta)\,,$$

$$\xi_{i,j}^n(z,r,\theta) = \beta_i^n J_n(k_i^n r) e^{in\theta} \sin(K_j z) \qquad (eq.9)$$

where $k_i^n R$ is the i^{th} zero of the Bessel function of integer order $J_n(x)$, $K_j = j\pi/Z_c$ and the normalization factor β_i^n is given by

$$\beta_i^n = \sqrt{\frac{8}{V}} \frac{1}{|\, J_{n-1}(k_i^n R) - J_{n+1}(k_i^n R)\,|} \qquad (Eq.10)$$

and V is the volume of the cylinder $\pi Z_c R^2$. For each value n, the Hamiltonian is diagonalized and yields a family of solutions. The matrix elements are given by:

$$< \xi_{i,j}^n \mid H_z \mid \xi_{l,m}^n > = \frac{\hbar^2 K_j K_m}{2} \beta_i^n \beta_l^n \int_0^R 2\pi r dr J_n(k_i^n r) J_n(k_l^n r) F_{j,m}(r), \qquad (Eq.11)$$

$$F_{j,m}(r) = \int_0^{Z_c} dz \frac{\cos(K_j z)\cos(K_m z)}{m_e^z(z,r)} \qquad (Eq.12)$$

$$< \xi_{i,j}^n \mid H_{(r,\theta)} \mid \xi_{l,m}^n > = \frac{\hbar^2 k_i^n k_l^n}{2} \beta_i^n \beta_l^n \int_0^R 2\pi r dr [J_{n+1}(k_i^n r) J_{n+1}(k_l^n r) - J_{n-1}(k_i^n r) J_{n-1}(k_l^n r)] G_{j,m}(r), \qquad (Eq.13)$$

$$G_{j,m}(r) = \int_0^{Z_c} dz \frac{\sin(K_j z)\sin(K_m z)}{m_e^z(z,r)} \qquad (Eq.14)$$

$$< \xi_{i,j}^n \mid V_I(z) \mid \xi_{l,m}^n > = V_{InAs} \pi \beta_i^n \beta_i^l R^2 \left[J_{n+1}(k_i^n R)\right]^2 \delta_{i,l} O1_{j,m} \qquad (Eq.15)$$

$$O1_{j,m} = \int_{Z_2}^{Z_2+d} dz \sin(K_j z)\sin(K_m z) \qquad (Eq.16)$$

$$< \xi_{i,j}^n \mid V_{III}(z) \mid \xi_{l,m}^n > = V_{GaAs} \pi \beta_i^n \beta_i^l R^2 \left[J_{n+1}(k_i^n R)\right]^2 \delta_{i,l} \left(O2_{j,m} + O3_{j,m}\right) \qquad (Eq.17)$$

$$O2_{j,m} = \int_0^{Z_1} dz \sin(K_j z)\sin(K_m z) \qquad (Eq.18)$$

$$O3_{j,m} = \int_{Z_4}^{Z_c} dz \sin(K_j z)\sin(K_m z) \qquad (Eq.19)$$

$$< \xi_{i,j}^n \mid V_{II}(z) \mid \xi_{l,m}^n > = V_{InAs} \beta_i^n \beta_i^n \int_0^{r_c} 2\pi r dr J_n(k_i^n r) J_n(k_l^n r) P_{j,m}(r) \qquad (Eq.20)$$

$$P_{j,m}(r) = \int_{Z_2+d}^{Z_2+d+rc\tan(\alpha)-r\tan(\alpha)} dz \sin(K_j z)\sin(K_m z) \qquad (Eq.21)$$

$$< \xi^n_{i,j} \mid V_{IV}(z) \mid \xi^n_{l,m} >= \pi \beta^n_i \beta^l_i R^2 \left[J_{n+1}(k^n_i R) \right]^2 \delta_{i,l} O4_{j,m} \qquad (Eq.22)$$

$$O4_{j,m} = \int_0^{z_c} dz(-eFz)\sin(K_j z)\sin(K_m z) \qquad (Eq.23)$$

The calculation is done using a basis formed with 20 Bessel functions and 20 sine functions for each value of n and were done for two detectors with different well widths. The spectral photoresponse of the detector for sample A (having 110Å for the base and 65Å for the height) obtained at a bias of 1.8 volts (T=30K) using a Nicolet Nexus 870 FTIR. The peak is located at 123 meV. From our theoretical formulation, we associate the peak located at 123 meV to the transition from the fundamental state n=0 to the first excited state n=1. The calculated energy (132 meV) is in good agreement with the experimentally observed energy of 123 meV . The component of the operator momentum **p** perpendicular to the z axis commutes with the total hamiltonian of the system, and we can show that the optical selection rules in the dipole approximation for normal incidence is $\Delta n=\pm 1$, where n is the quantum number. Therefore in an ideal system, the transition from the quantum state n=0 to n=1 is allowed while the transition from n=0 to n=2 is forbidden.

To further corroborate our theoretical model, we calculated the transition energies in a different DWELL detector. From XTEM measurements, the quantum dots in this sample (sample B) were found to be pyramidal in shape with a base dimension of 140Å and 50 Å for the height. The photocurrent response measurements yielded a peak at 140 meV, which we associated to the transition from the ground state in the dot to the first excited state. Using the same theoretical model, we calculated the transition energy between the first excited state and the ground state to be 150 meV. This energy is in good agreement with the experimentally obtained value. Table 1 summarizes the different experimental and theoretical results obtained from the two photodetectors. The three lowest eigenvalues of sample B are calculated as a function of electric field. Figure 6 shows the variation of the three lowest energy levels as a function of the electric field for this sample. We see that the energy difference between the calculated energy levels does not change as a function of the electric field, this is in accord with experimental results. We should mention that the electron energy levels are strongly dependent on the direction of the electric field, reflecting the fact the structure is not symmetric along the growth direction, i.e. the absence of spatial reversal symmetry due to the shape of the quantum dot.

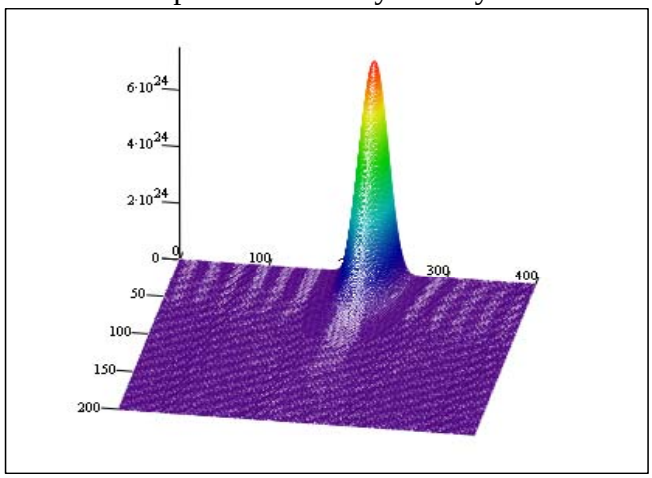

Figure 2: Calculated profile of the wavefunction ($|\Psi|^2$) for the ground state in the quantum dots in a well heterostructure. The arrows indicate the position of the quantum dots in the radial and z directions.

Our experimental and theoretical results show that the energy spacing between the first excited state and the fundamental state is much larger than the confined longitudinal optical

phonon energy (~30 meV). This is expected to result in a longer carrier lifetime for the carriers in the excited state, which in turn would increase the quantum efficiency of the detector due to the higher escape probability of the photoexcited carriers. Figure 2 shows the square of the wavefunction corresponding to n=0 obtained under zero electric field conditions. It was observed that the wavefunction of the fundamental state is well localized inside the quantum dot. We changed in our model the dimensions of the dots by ± 10 % and we found the energy transition to change by ± 20%, which is still in good agreement with the experimental results.

In conclusion, we have undertaken theoretical modeling and experimental characterization of a novel InAs/InGaAs DWELL heterostructure. The calculation of the energy levels and wavefunction in this system is obtained using a Bessel functions expansion approach. From the theoretical formulations, we have been able to associate the peak obtained in the spectral response of the detector. Reasonably good agreement between the experimental and the theoretical results has been obtained for two different DWELL structures.

Carrier Dynamics in DWELL System

Carrier dynamics in self-assembled quantum dots (QD) has been a subject of active research in the past few years. Because of the discrete nature of the confined electronic energy levels and phonon energies in the QDs, various interesting phenomena such as the "phonon bottleneck", which refers to the dramatic reduction in the intersubband relaxation time have been predicted[1,2]. The phonon bottleneck can limit the maximum modulation bandwidth of quantum dot lasers, while proving to be beneficial for intersubband QD detectors[3]. Time resolved photoluminescence has been used by different research groups to measure the carrier lifetimes in QDs[4-7]. Pump-probe spectroscopy has also used to measure the carrier relaxation times in QDs.[8-14] The fast carrier relaxation time has been explained by the presence of electron-hole scattering and multiple optical phonon emission[10,13]. Recently, resonant pump probe spectroscopy was used to estimate the intersubband relaxation times in self assembled QDs using the Dutch free-electron laser[15]. In our research group, we are investigating infrared lasers and detectors fabricated using a novel heterostructure called quantum dots in a well (DWELL) design. In this structure, InAs QDs are positioned in a thin InGaAs quantum well, which in turn is placed in a GaAs matrix. This design has resulted in a significant technological advancement since the DWELL design increases carrier collection efficiency in interband lasers[16] and reduces thermionic emission and provides better control over the operating wavelength in intersubband detectors[17]. Moreover, the DWELL system also has inherently rich physics since the photoexcited (or electrically injected) carriers are unconfined in the GaAs barrier, relax into a 2-dimensional quantum well (QW) and finally get trapped in a quasi-zero dimensional QDs. To the best of our knowledge, there has been no report on the investigation of carrier lifetimes in the DWELL system. We have reported the measurement of carrier dynamics in the DWELL system using non-degenerate pump probe spectroscopy. In this measurement, carriers are created in the GaAs barrier using pump laser and the number of carriers in the ground state of the dot was obtained by measuring the differential transmission (DT) of a delayed probe. Using this approach, the intersubband (τ_{intra}) and interband (τ_{inter}) lifetimes were found to be 2.5 ps and 700ps at 77K and 5.0 ps and 650 ps at room temperature. It is interesting to note that that τ_{intra} (defined as the time taken for the carrier to relax from the GaAs barrier to the ground state of the dot) increases as a function of temperature, whereas τ_{inter} (defined as the recombination time of the carriers in the ground state of the dot) decreases as a function of the temperature.

The InAs/InGaAs DWELL detectors were grown by solid source molecular beam epitaxy (MBE). The substrate temperature was 590ºC during the growth of GaAs buffer layer and lowered to 475ºC during the growth of InAs quantum dots. The active region consists of 10 periods of 60Å $In_{0.15}Ga_{0.85}As$, 2.4 monolayers of InAs, 60Å of $In_{0.15}Ga_{0.85}As$ and 490 Å of GaAs. The InAs layers are doped with silicon with a concentration of ~5 x 10^{10} atoms/cm^2. The growth rate for the InAs layer is 0.05ML/s. The dot density is estimated to be ~ 5*10^{10} cm^{-2} using atomic force microscopy (AFM) and were found to be hemispherical using cross sectional transmission electron microscopy (X-TEM). The bandstructure of the DWELL heterostructure was theoretically modeled using a single band k.p model and the calculated bandstructure is shown in Fig.1[18]. It is to be noted that the interband transition from the electron ground state to the hole ground state is estimated to be at 1.0 eV (λ ~1.24 μm). This was verified using photoluminescence (PL) measurements obtained using a 775nm pulsed Ti:sapphire pump laser. (as shown in Fig. 4). The peak at 1150 nm is attributed to the ground state transition whereas the 1030nm peak is associated with the higher lying states in the DWELL. The PL peak under low excitation conditions is around 1.2 μm, in good agreement with the theoretical model. The blue shift under higher excitation conditions is probably due to band filling effects.

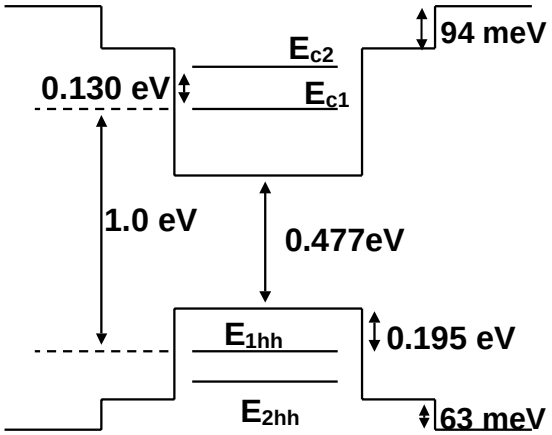

Figure 3: Calculated energy band diagram using a single band k.p model, showing the various energy levels in the quantum dots in a well (DWELL) heterostructure

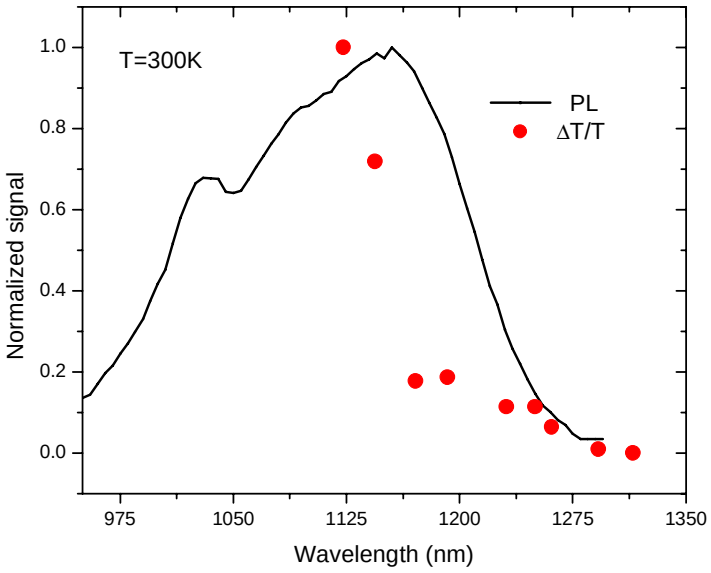

Figure 4: Photoluminescence (PL) and differential transmission (DT) spectra of the DWELL sample. The PL peak at 1150 nm is attributed to the ground state of the QD, whereas the peak at 1030 nm is probably due to a higher lying state in the DWELL. Note that the DT spectra follows the long wavelength tail of the PL spectrum.

To further corroborate the position of the ground state of the DWELL, DT measurements were undertaken. In order to remove any contribution from the substrate, the substrate was thinned first by mechanical polishing and the rest of it removed using selective chemical etching. In the DT measurement, the optical output of a mode-locked Ti:sapphire laser (Clark CPA 2001) generating 200 fs laser pulses at 775nm with a repetition rate of 1 kHz was used as the pump beam. The output power of the Ti:sapphire laser was 900 mW of which 50 mW was used to pump the sample and 850 mW was used to pump a Clark IOP-1012 optical parametric amplifier (OPA). The output from the OPA, which was used as the probe, was tunable from 1130 nm to 2500nm. The pump was chopped at 100Hz and the differential change in the transmission of the probe was measured with an InSb detector and a lock-in amplifier. The differential transmission signal $\Delta T/T$ is defined as :

$$\frac{\Delta T}{T} = 1 - e^{-\Delta\alpha d} \approx \Delta\alpha \cdot d \quad ; \quad \Delta\alpha \cdot d << 1 \qquad (Eq.1)$$

where $\Delta\alpha$ is the induced absorption by the pump and d is the thickness of the active region. The DT signal is a measure of the number of carriers in the given state since a higher number of carriers would translate into a higher absorption. The wavelength of the probe was tuned from 1130 nm to 1320 nm and the measured DT signal is shown in Fig. 5. The DT signal follows the long wavelength tail of the PL spectrum and falls to zero beyond 1300 nm indicating that the DT signal arises because of transitions in the ground state of the QD.

Time dependent DT measurements were then undertaken at 77K and 300K using the 775 nm pump to create carriers in the GaAs barrier and a delayed probe tuned to the ground state of the QD to measure the number of carriers in this state. The optical excitation density of the probe and the pump are $200\mu J/cm^2$ and $6mJ/cm^2$, respectively. For comparison purposes, measurements were undertaken on a reference GaAs substrate and a negative DT signal was obtained, possibly due to induced absorption by defect states. The signal from the DWELL sample had a DT spectrum very different from that obtained with the substrate, confirming that the signal was arising from the DWELL active region. Figure 3 shows the rise time of the DT signal as a function of the delay at 77K and 300K for the DWELL sample. As shown in the inset to Fig. 3, the rise time of the DT signal corresponds to intersubband relaxation time (τ_{intra}), which is defined as the amount of time needed for the carriers to relax from the GaAs barrier to the QD ground state. If we assume that the holes relax fairly quickly as corroborated by Sosnowski et al[13], who measured a hole intersubband relaxation time to be about 600 fs, τ_{intra} can be attributed to the electrons and a simple exponential fit can be used to extract τ_{intra},

$$\frac{\Delta T}{T} = C(1 - e^{-t/\tau_{intra}}) \qquad (Eq.2)$$

Using this approach, we find that τ_{intra} = 2.5 ps at 77K and increases to 5 ps at 300K. If phonon scattering were the dominant intersubband scattering mechanism, then the carrier lifetime would decrease at higher temperatures due to increased scattering. The empirically observed trend indicates that alternative relaxation mechanisms such as electron-hole scattering[9] or Auger like scattering[10] become activated. Since our excitation intensity is fairly large (~50 electron-hole pairs per dot), it is reasonable to assume that these carrier-carrier scattering mechanisms become dominant channels for carrier relaxation, under these conditions.

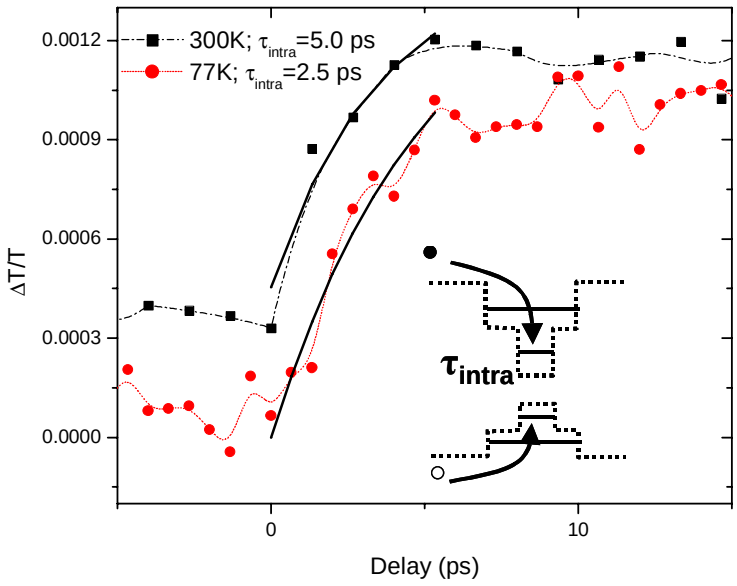

Figure 5: The differential transmission signal as function of delay obtained using a 775 nm pump and a probe tuned to the ground state of the dot. The rise time of the signal is a measure of the intersubband relaxation time, i.e. duration of time for the carriers to relax from the GaAs barrier to the ground state of the QD, as shown in the inset.

By observing the decay of the DT signal, we can get an estimate of the interband recombination time in the DWELLs, τ_{inter}, which is defined as the recombination lifetime of carriers in the ground state of the QD as shown in the inset to Fig. 5. A simple exponential decay fit of the data yields τ_{inter} = 700 ps at 77K and it decreases to 650ps at 300K. This is in good agreement with recombination lifetimes reported in QDs obtained using time resolved photoluminescence measurements[19].

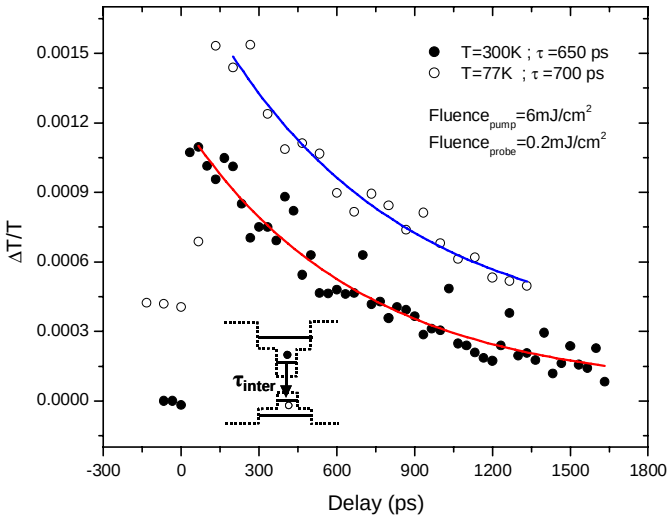

Figure 6: The decay of the differential transmission signal as function of delay obtained using a 775 nm pump and a probe tuned to the ground state of the dot. The fall time of the signal is a measure of the interband relaxation time, i.e. the recombination lifetime of the ground state of the QD, as shown in the inset.

In conclusion, we have undertaken non-degenerate pump-probe spectroscopy to study the carrier dynamics in a novel InAs/InGaAs quantum dots in a well (DWELL) heterostructure. Using a pump to create carriers in the barrier and a delayed probe tuned to the ground state of the dot, the intersubband and interband relaxation time were extracted. At 77K (300K), the intersubband lifetime was found to be 2.5 ps (5 ps) and the interband lifetime was found to be 700 ps (650 ps). This fast intersubband relaxation is attributed to electron-hole and other Auger like processes. We are currently investigating the effect of the fluence on the carrier dynamics in the DWELL system.

Peer Reviewed Journal Papers

1. P. Hill, N. Weisse-Bernstein, L. R. Dawson, P. Dowd, and S. Krishna, "Activation energies for Te and Be in metamorphically grown AlSb and InxAl1–xSb layers", Appl. Phys. Lett. **87**, 092105 (2005)
2. G. Balakrishnan, S.H. Huang, A. Khoshakhlagh, P. Hill, A. Amtout, S. Krishna, G.P. Donati, L.R. Dawson and D.L. Huffaker, IEE Electronics Letters, Vol. 41, No. 9, pg 531, 2005.
3. A. Amtout, S. Raghavan, P. Rotella , G. von Winckel, A. Stintz and S. Krishna "Theoretical Modeling And Experimental Characterization of InAs/InGaAs Quantum Dots In a Well Detector, *Journal of Applied Physics*, October 2004.
4. G. von Winckel, E. A. Coutsias and S. Krishna, "Spectral Element Modeling of Semiconductor Heterostructure', Manuscript in Preparation.
5. S. Raghavan, D. Forman, P. Hill, N. W- Bernstein, G. von Winckel, P. Rotella, S. Krishna, S. W. Kennerly and J. W. Little, "Normal-Incidence InAs/InGaAs Quantum Dots-in-a-Well Detector Operating in the Long Wave Infrared Atmospheric Window, *Journal of Applied Physics* **96**, 1036 (2004).

References

1. H. Bensity, C. M. Sotomayor-Torres, and C. Weisbuch, *Phys. Rev. B* **44**, 10945(1991)
2 . U. Bockelmann and G. Bastard, *Phys. Rev. B* **42**, 8947 (1990)
3 P. Bhattacharya, S. Krishna, J. Phillips, P. J. McCann and K. Namjou , *J. Crystal Growth*, **227**, 27, 2001.
4 L. Zhang, Thomas F. Boggess, D. G. Deppe, D. L. Huffaker, O. B. Shchekin, and C. Cao, *Appl. Phys. Lett* **76**, 1222, (2000)
5 B. Ohnesorge, M. Albrecht, J. Oshinowo, A. Forchel, and Y. Arakawa, *Phys. Rev. B* **54**, 11532, (1996)
6 S. Raymond, S. Fafard, P. J. Poole, A. Wojs, P. Hawrylak, S. Charbonneau, D. Leonard, R. Leonard, R. Leon, P. M. Petroff, and J. L. Merz, *Phys. Rev. B* **54**, 11548, (1996)
7 F. Adler, M. Geiger, A. Bauknecht, F. Scholz, H. Schweizer, M. H. Pilkuhn, B. Ohnesorge, and A. Forchel, *J. Appl. Phys.* **80**, 4019, (1996)
8 K. Kim, J. Urayama, T. B. Norris, J. Singh, J. Phillips, and P. Bhattacharya, *Appl. Phys. Lett*. **81**, (2002) 670.
9 J. Urayama, T. B. Norris, H. Jiang, J. Sing, and P. Bhattacharya, *Appl. Phys. Lett* 80, 2162, 2002
10 J. Feldman, S. T. Cundiff, M. Arzberger, G. Bohm, and G. Abstreiter, *J. Appl. Phys*., **89**, 2001
11 D. Birkedal, J. Bloch, J. Shah, L. N. Pfeiffer, and K. West, *Appl. Phys. Lett*., **77**, 2201, 2000
12 F. Quochi, M. Dinu, J. Shah, L. N. Pfeiffer, K. W. West, and P. M. Platzman, *Phys. Rev. B*, **65**, 161038, 2002
13 T. S. Sosnowski, T. B. Norris, H. Jiang, J. Singh, K. Kamath, and P. Bhattacharya *Phys. Rev. B* **57**, 9423, 1998
14 Dzmitry A. Yarotski, Richard D. Averitt, Nicolas Negre, Scott A. Crooker, Antoinette J. Taylor, Giovanni P. Donati, Andreas Stintz, Luke F. Lester, and Kevin J. Malloy, *J. Opt. Soc. Am. B* **19**, 1480 (2002)
15 . E. A. Zibik, L. R. Wilson, R. P. Green,G. Bastard, R. Ferreira, P. J. Phillips, D. A. Carder, J-P. R. Wells, J. W. Cockburn, M. S. Skolnick, M. J. Steer, and M. Hopkinson, *Phys. Rev. B*, **70**, (2004) 161305
16. G.T. Liu, A. Stintz, H. Li, K.J. Malloy, and L.F. Lester *Electron. Lett*. **35**, 1163 (1999)
17 S. Krishna, S. Raghavan, G von Winckel, A. Stintz, , G. Ariyawansa, S.G. Matsik and A.G.U. Perera, *Appl. Phys. Lett*., **83**, 2745, (2003).
18 A. Amtout, S. Raghavan, P. Rotella, G. von Winckel, A. Stintz, and S. Krishna, *J. Appl. Phys.* **96**, 3782 (2004)
19 K. Kamath, N. Chervela, K. K. Linder, T. Sosnowski, H-T. Jiang, T. Norris, J. Singh, and P. Bhattacharya *Appl. Phys. Lett*. **71**, 927 (1997)